BIOTROPICA
THE JOURNAL OF THE ASSOCIATION FOR TROPICAL BIOLOGY AND CONSERVATION

BIOTROPICA 50(3): 374–383 2018 10.1111/btp.12522

Solar irradiance as the proximate cue for flowering in a tropical moist forest

S. Joseph Wright[1] and **Osvaldo Calderón**

Smithsonian Tropical Research Institute, Apartado 0843–03092, Balboa, Republic of Panama

ABSTRACT

We compared flowering times predicted by six possible proximate cues involving seasonal changes in rainfall and irradiance and flowering times observed over 30 years of weekly censuses for 19 tree and liana species from Barro Colorado Island (BCI), Panama. Hypotheses concerning variation in the timing and intensity of rainfall failed to predict flowering times in any species. In contrast, 10 to 12 weeks of consistent high levels of irradiance predicted flowering times well for eight species, and six or seven weeks of rapidly increasing levels of irradiance predicted flowering times well for two species. None of the six possible proximate cues predicted flowering times adequately for the nine remaining species. We conclude that high and increasing levels of irradiance are the proximate cues for flowering in many BCI species. The seasonal movements of the Intertropical Convergence Zone cause strong seasonal changes in cloud cover, atmospheric transmissivity, and irradiance reaching the BCI forest. Inter-annual variation in the timing of movements of the Intertropical Convergence Zone is the most likely cause of inter-annual variation in the timing of flowering in these species. Much work remains to be done as the physiological mechanisms linking flowering and irradiance are unknown and the proximate cues for flowering remain to be identified for many other BCI species.

Abstract in Spanish is available with online material.

Key words: Barro Colorado Island; flowering times; moisture availability; phenology; rainfall; solar insolation.

The proximate environmental cues that initiate flowering are well documented at temperate and boreal latitudes but remain a matter for conjecture and hypotheses at tropical latitudes. At temperate and boreal latitudes, proximate cues for flowering include seasonal changes in photoperiod, winter vernalization and growing degree days; genetic mechanisms that link these cues to flowering are well documented in model organisms; and models that relate climate change scenarios and the genetic responses that control flowering are now possible (Satake *et al.* 2013). In contrast, a limited number of experiments and a welter of mostly vague hypotheses relate flowering and proximate environmental cues in the tropics.

Classical experiments conducted in the tropics demonstrate that proximate cues for flowering can include changes in photoperiod of just 10 min in rice (Njoku 1959), short temperature dips associated with rainstorms in orchids (reviewed by Wycherley 1973) and irrigation following drought in coffee (reviewed by Carr 2001) and several other forest plants (Augspurger 1982, Reich & Borchert 1982). Similar experiments are rarely possible for the large trees and lianas that dominate tropical forest canopies and are always difficult to interpret because many environmental parameters change simultaneously in nature and these simultaneous changes have not been recreated experimentally at the large spatial scales of forest trees. We are left with long-term observational studies and correlations between the timing of flowering and hypothesized proximate cues.

Long-term observational studies have related the timing of flowering to short temperature dips (*e.g.*, Ashton *et al.* 1988, Tutin & Fernandez 1993), seasonally sufficient levels of moisture availability (*e.g.*, Reich & Borchert 1984), prior drought followed by rain (*e.g.*, Sakai *et al.* 2006), levels of solar irradiance at the forest canopy (van Schaik *et al.* 1993, Wright & van Schaik 1994, Yeang 2007), levels of solar insolation at the top of the atmosphere (Calle *et al.* 2009, 2010, Borchert *et al.* 2015), and photoperiod (reviewed by Wycherley 1973). The specific proximate cue—the required level and duration of the environmental signal—is rarely, if ever known because observational studies tend to be short, flowering tends to be infrequent, and too few flowering events are observed to refine understanding of the proximate cue. As one example, Yeang (2007, p. 288) wrote: "The specific attributes of high solar radiation that are critical to synchronous flowering still need to be determined: whether it is the average solar radiation received that is important or if it might be, for example, very high radiation on a few cloud-free days, or the hours of high daily sunshine that are also relevant." Our goal is to fill in such specifics.

We have accumulated a 30 yr record (1987 through 2016) of weekly censuses for the presence of flowers identified to species in 200 litter traps on Barro Colorado Island (BCI), Panama. Most flowers last a single day in humid, lowland tropical forests (Primack 1985), so arrival in litter traps closely represents flowering times. We will compare observed first flowering dates with

Received 22 April 2017; revision accepted 2 October 2017.

[1]Corresponding author; e-mail: wrightj@si.edu

predictions of seven models structured to represent seven possible proximate cues involving rainfall, solar irradiance, and photoperiod or top-of-the-atmosphere insolation. We parameterize rainfall and irradiance models with daily values measured just above the forest canopy on BCI. We then search parameter space to identify the model that best predicts observed first flowering dates. We find evidence consistent with the hypotheses that sustained high levels of solar irradiance or sustained increases in irradiance at the forest canopy act as proximate cues for flowering in 10 of the 19 species evaluated.

METHODS

Study site.—BCI (9° 10′ N, 79° 51′ W) supports tropical moist forest in the Holdridge Life Zone System. Annual rainfall averages 2600 mm, with 10 percent of the annual total falling during a four-month dry season. Temperatures average 26°C for 11 months of the year and 27°C in April, the final month of the dry season. This study took place in primary, old growth forest with a 30- to 35-m tall canopy within the 50-ha Forest Dynamics Plot (Condit *et al.* 2012). Leigh (1999) further describes BCI.

Meteorological variables.—We measured rainfall manually with a rain gauge (NovaLynx 26-2510, Auburn, CA, USA) in the laboratory clearing and electronically with a tipping bucket (Li-Cor 1400-106, Lincoln, NE, USA) mounted on a tower above the forest canopy. We used manual daily rainfall, filling holes with prorated values recorded by the tipping bucket. We measured global solar irradiance with a pyranometer (Li-Cor Silicon Pyranometer, Lincoln, NE, USA) mounted on top of the same tower. We recorded solar radiation (W/m^2) every 15 min and integrated to daily totals (MJ/m^2). There were 319 missing daily totals between 1 January 1986 and 9 March 2017. We filled these missing values with seven-day running means (Fig. 1) calculated using mean values for each day of the year. The tower was extended from 42 m to 48 m in 2006. The top of the forest canopy was more than 2 m below the sensors before 2006 so the move should not have affected measurements. Detailed information about instrumentation, calibration, and location changes can be found at https://repository.si.edu/handle/10088/29560 (https://doi.org/10.5479/data.stri/10088/29560).

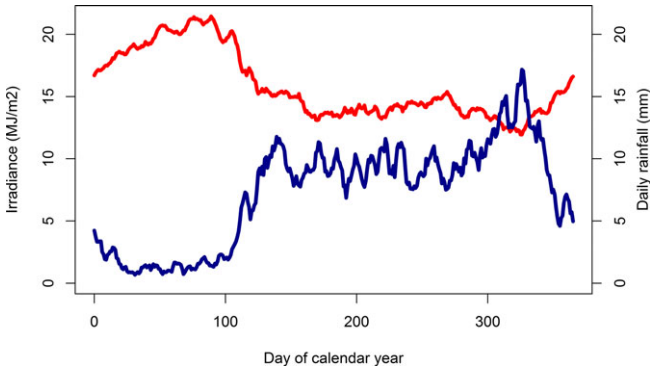

FIGURE 1. Total daily irradiance (red line) and rainfall (blue line) on Barro Colorado Island, Panama. Daily mean values were calculated for each day of the calendar year, using records from 1 January 1986 to 9 March 2017. Lines represent seven-day running averages of these daily mean values.

Phenological censuses and the response variable.—We identified all plant reproductive structures captured in 200 passive traps to species, each week, from 5 January 1987 through 27 December 2016. We recorded the presence of flowers starting with the fifth census (3 to 9 February 1987). Each trap had a surface area of 0.5 m^2 composed of a loose, 1-mm mesh bag of plastic-coated fiber glass window screen suspended 80 to 100 cm above the ground from a PVC frame. The traps were located at 13.5-m intervals on alternating sides and 4 to 10 m from pre-existing trails. Wright and Calderon (1995, 2006) provide further details.

Our response variable was the median first census traps recorded flowers for each species-specific phenological year. We chose median first censuses because individuals occasionally produce small numbers of flowers at unusual times on BCI (Fig. S1), and medians are relatively insensitive to these rare events. Species-specific phenological years began on the date that corresponded to the minimum of 365 variances obtained by linearizing flowering dates to a 1 to 365 scale, moving day 1 to each of the 365 possible days of the year, and calculating a variance of flowering dates for all 365 possible values of day 1. The midpoint was chosen when consecutive days of the year had identical flowering variances. In practice, the species-specific phenological years begin near the midpoint of those consecutive days of the calendar year lacking flowers (see Figs 2 and S1).

First flowering times always risk a late bias. To minimize late bias, we excluded species with fewer than 1500 flower records, where each species-trap-census combination constitutes a flower

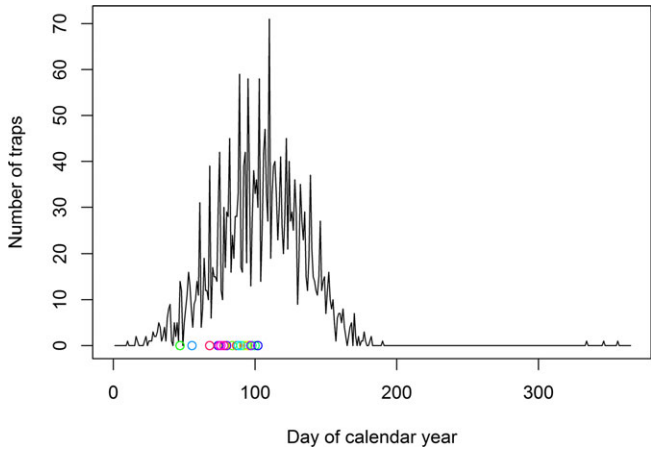

FIGURE 2. The seasonal timing of flowering of *Gustavia superba*. The black line represents the number of litter traps that captured flowers for each day of the calendar year summed over 1561 weekly censuses (9 February 1987 through 27 December 2016). The colorful open symbols represent median first flowering censuses for 28 years. Figure S1 presents the same information for all 19 study species.

record. To ensure that many flowering individuals were under study, we also excluded species recorded from fewer than 30 traps. We evaluated histograms of flower records by day of year over the entire record (Figs 1 and S1) for species that met these two criteria and excluded species that flowered continuously or with multiple peaks because our response variable, median first flowering census, lacks meaning for continuously and multiple flowering species. A final minimum sample size requirement concerned the number of different traps for each species in each phenological year (Fig. S2). We set this final requirement at 10 traps; however, we had to relax this final requirement occasionally because flowering levels vary widely among years on BCI (Wright & Calderon 2006) and several species with otherwise rich flowering data nearly failed to flower in one or two years (see *Results: Phenological censuses*).

PHENOLOGICAL HYPOTHESES AND ANALYSES.—We will predict the first flowering census for each species for each species-specific phenological year for seven hypothesized proximate cues. Our censuses are numbered linearly (1 to 1561) so that the circular nature of time (*i.e.*, 1 January follows 31 December) is not an issue. We now describe how each hypothesis generates predicted first flowering censuses.

The simplest model hypothesizes that flowering begins on a critical day of the calendar year (DOY_{crit}). Both photoperiod and top-of-the-atmosphere insolation vary seasonally but not interannually and, as proximate cues for flowering, should be associated with flowering near a particular day of the year. The day-of-year model predicts flowering is initiated on DOY_{crit} each year, with flowers developing and falling into traps on a fixed date each year.

The six remaining models hypothesize that flowering begins N_d days after the first time an environmental signal accumulated over the previous N_e days exceeds a threshold (T) during each species-specific phenological year. N_d and N_e capture the time flowers take to develop and the window of time over which an environmental signal accumulates, respectively. We use N_d, N_e, and BCI meteorological records (see *Methods: Meteorological variables*) to calculate environmental signals (E_d) for each of the 10,921 days between our first and final censuses. Meteorological years began on fixed dates as often used in thermal time models for temperate and boreal plants (Linkosalo *et al.* 2008). For rainfall, meteorological years began in early January, which marks the beginning of the dry season (Fig. 1). For solar irradiance, meteorological years began in late October, which is the cloudiest time of year (Fig. 1). If high or increasing levels of rainfall break drought and this triggers flowering, those rains must occur during or after the dry season (*i.e.,* after early January). If high or increasing levels of irradiance relieve light limitation and this triggers flowering, the improving irradiance must follow the annual maximum in cloud cover and minimum in irradiance (*i.e.*, after late October) in the strictly annually flowering species considered here.

The definition of E_d distinguishes three rainfall and three irradiance hypotheses. For each hypothesis, flowering is predicted to begin during the first census for which E_d exceeds T for each species-specific phenological year. We evaluated three environmental signals for irradiance and for rainfall. The three signals concern mean levels, maximum levels, and directional change of the environmental signal. For mean and maximum levels, we calculate E_d as follows:

$$E_d = \left(\sum_{t=d-N_d-N_e}^{t=d-N_d} V_t \right) / N_e$$

where V_t is the value of rainfall (mm) or total irradiance (MJ/m^2) on day t and E_d is the mean value of V_t between days d-N_d and d-N_d-N_e. For each census, we calculated mean and maximum values of E_d from the day of the previous census to the day before the current census. Hypotheses concerning mean and maximum levels differ because flowering is predicted to begin during the first census for which the census-specific mean or maximum value of E_d exceeds T, respectively. In practice, the mean and maximum values of E_d tend to converge for large values of N_e (because E_d is a mean over N_e days), but can be very different for small values of N_e.

For the directional change hypothesis, we calculate the environmental signal for each day as follows:

$$E_d = \sum_{t=d-N_d-N_e}^{t=d-N_d} \left(V_t - \overline{V}\right) \times (t - \overline{t}) / \sum_{t=d-N_d-N_e}^{t=d-N_d} (t - \overline{t})^2$$

where $\overline{V}$ and $\overline{t}$ are mean values over the relevant days and E_d is the slope of the relationship between the environmental signal and Julian day. Note that Julian day is on a linear scale, which technically started on 1 January 4713 BC (https://en.wikipedia.org/wiki/Julian_day). Flowering is predicted to begin during the first census for which the mean of the daily values of E_d exceeds T, where the mean is again calculated from the day of the previous census to the day before the current census.

Parameter sets included all combinations of N_e, N_d, and T for the six hypotheses concerning rainfall and solar irradiance. N_d took all integer values between 1 and 210 days for all six hypotheses. This range of N_d values allows flowers to develop in a single day, which might occur if the proximate cue triggers anthesis of resting buds, or in seven months, which might occur if the proximate cue triggers differentiation of reproductive buds. We capped N_d at seven months because, for most BCI species and all 19 study species, inflorescences develop distal to the newest leaves (see photographs in Croat 1978, SJW, personal observations), new leaves are produced at the transitions from dry-to-wet and wet-to-dry seasons (Leigh & Windsor 1982, Aide 1993), and this caps N_d at four and seven months for dry- and wet-season flowering species, respectively. In practice, all reasonable fits between predicted and observed flowering times were associated with values of $N_d \leq 107$ days (Tables 2 and 3).

N_e took all integer values between 1 and 125 days for hypotheses concerning mean and maximum values and between 1 and 60 days for hypotheses concerning directional change of environmental signals. The range of N_e values for hypotheses concerning mean and maximal values allows E_d to exceed T in a

single day, which might occur if the proximate cue was a heavy dry-season rain, or in four months, which might occur if the proximate cue was irradiance over the entire dry season or rainfall over the first half of the rainy season. In practice, all reasonable fits between predicted and observed flowering times were associated with values of $N_e \leq 98$ days for hypotheses concerning means and maxima (Tables 2 and 3). The range of N_e values for hypotheses concerning directional change had a hard upper bound of 60 days because directional change in rainfall and irradiance is never sustained for more than 60 days on BCI (Fig. 1).

T took the following hypothesis-specific values:

1. between 15 and 21.75 with 0.25 MJ/m^2 steps for mean irradiance, where 15 MJ/m^2 is larger than mean values during the cloudy, rainy season and 21.75 MJ/m^2 is the largest mean value observed (Fig. 1),
2. between 16 and 22.25 with 0.25 MJ/m^2 steps for maximum irradiance, where 16 and 22.25 MJ/m^2 span the range of sustained maximum irradiance observed early and late in most dry seasons,
3. between 0.08 and 0.22 with 0.01 $MJ/m^2/d$ steps and between 0.25 and 1.00 with 0.05 $MJ/m^2/d$ steps for directional change in irradiance, where 0.08 and 1.00 $MJ/m^2/d$ span the range of increasing irradiance observed for different values of N_e,
4. between 5.0 and 11.1 mm with 0.1 mm steps for mean daily rainfall, where 5 mm approximates daily evapotranspiration and 11.1 mm approximates mean daily rainfall in the rainy season (Fig. 1),
5. between 5 and 20 mm with 1 mm steps and between 22 and 80 mm with 2 mm steps for maximum daily rainfall, where 5 mm approximates daily evapotranspiration and 80 mm captures >99 percentage of rainfall events, and
6. between 0.2 and 4.0 with 0.1 mm/d steps for directional change in rainfall, where 0.2 and 4.0 mm/d span the range of increasing rainfall observed for different values of N_e.

DOY_{crit} is the only parameter for the day-of-year hypothesis and took all 365 possible values.

We calculated the population root-mean-square error (RMSE) between predicted and observed census numbers for each parameter set, where

$$\text{RMSE} = \sqrt{\sum_y \left(p_y - o_y\right)^2 / n},$$

n is the number of years and p_y and o_y are the predicted and observed first census numbers for year y, respectively. There was no predicted census number for year y if E_d failed to exceed T. We calculated RMSE for all parameter sets, but only consider parameter sets with predicted census numbers in 27 or more years for these strictly annually flowering species. RMSE units are census intervals, which correspond closely to weeks (see *Results: Phenological censuses*). The interpretation of our results hinges on minimum RMSE values and whether the associated parameter values are biologically reasonable. An RMSE value of 1.5 indicates that 69 percent of predicted first flowering dates fall within 1.5 censuses or approximately 1.5 weeks of observed first flowering dates. We will take this as strong evidence that a hypothesized proximate cue is consistent with observed flowering times and consider RMSE values up to 2 as weak evidence. Finally, we evaluated the hypotheses associated with the 1000 smallest RMSE values for each species.

RESULTS

Phenological censuses and study species.—We recorded 264,988 flower records in 1561 weekly censuses. Nineteen focal species fulfilled the criteria described in *Methods: Phenological censuses and the response variable*, although the requirement that each species was captured in 10 different traps in each phenological year, was relaxed for 13 of 547 combinations of species and phenological year involving eight of the 19 focal species (see Fig. S2 for details).

The 19 study species include a representative cross section of the more abundant woody species of central Panama. They include 16 families, 17 genera, 12 evergreen and seven deciduous species, four liana species, and 15 free-standing species ranging from understory shrubs and treelets to the largest canopy trees (Table 1). Median first flowering dates occur one, two, and six to eight months after last being deciduous for *Alseis blackiana, Dipteryx oleifera,* and the five remaining deciduous species, respectively. All 19 species are locally abundant as reproductive adults, although several light-demanding species are poorly represented as juveniles and have relatively few individuals in the 50-ha plot for this reason (Wright *et al.* 2003).

We recorded 66,751 flower records for the 19 focal species (Table 1). We discarded the first and final phenological year if any trap first captured a species within four censuses of the first or final censuses conducted on 9 February 1987 and 27 December 2016, respectively. For this reason, we recorded 28, 29, or 30 flowering phenological years for different focal species (Table 1).

Census interval length affects the interpretation of RMSE values. Census interval lengths (number of intervals) were 4 (3), 5 (29), 6 (259), 7 (982), 8 (247), 9 (35), 10 (3), 12 (1), 14 (1), and 17 (1) days. The longest, 17-day interval occurred while BCI was evacuated when the United States invaded Panama in 1989. The remaining 4-day and 10- to 14-day intervals coincided with planned holidays or unexpected illnesses. We will interpret RMSE units as weeks because 95.3 percent of census intervals were from 6 to 8 days, which corresponds closely to weekly intervals.

Phenological hypotheses.—Tables 2 and 3 present minimum RMSE values and associated parameter values for each species for the seven phenological hypotheses. Species-specific minimum RMSE values rarely differ by more than one unit for the day-of-year hypothesis and the three irradiance hypotheses (Table 2). All minimum RMSE values were much larger for the three rainfall hypotheses (Table 3).

TABLE 1. *Descriptions of the 19 focal species, sample sizes, and inter-annual ranges of first flowering dates.*

						Sample size this study[e]			Median first flowering day-of-year[f]	
Code	*Species*[a]	Family	Leaf habit[b]	Life form[c]	Stems per 50 ha[d]	Record	Traps	Years	First	Last
ALSB	*Alseis blackiana*	Rubi-	DF	T	8,263	2,322	123	30	90	145
BEIP	*Beilschmiedia pendula*	Laur-	E	T	2,140	1,823	61	29	321	4
CORA	*Cordia alliodora*	Boragin-	DF	T	146	3,407	175	29	47	81
CORB	*Cordia bicolor*	Boragin-	DF	M	653	2,217	67	28	34	73
CORL	*Cordia lasiocalyx*	Boragin-	DB	U	1,163	2,136	80	29	50	77
DIPP	*Dipteryx oleifera*	Fab-	DB	T	51	6,898	124	30	139	205
FARO	*Faramea occidentalis*	Rubi-	E	U	26,121	7,797	174	29	101	170
GUSS	*Gustavia superba*	Lecythid-	E	U	762	2,692	37	28	47	102
HIR1	*Hiraea reclinata*	Malpighi-	E	L	354	2,926	177	28	9	130
HYBP	*Hybanthus prunifolius*	Viol-	E	S	30,208	1,898	129	29	66	124
JACC	*Jacaranda copaia*	Bignoni-	DB	T	279	4,411	123	29	31	99
LUE1	*Luehea seemannii*	Tili-	DF	T	185	4,517	95	28	356	43
MARP	*Maripa panamensis*	Convolvul-	E	L	2,961	3,532	130	29	47	92
PRIA	*Prionostemma asperum*	Celastr-	E	L	3,213	3,421	100	29	26	80
SIMA	*Simarouba amara*	Simaroub-	E	T	1,482	1,929	61	29	27	66
TABA	*Tabernaemontana arborea*	Apocyn-	E	T	1,620	7,278	87	28	26	106
THIM	*Thinouia myriantha*	Sapind-	E	L	1,398	2,608	119	29	5	51
TRIC	*Triplaris cumingiana*	Polygon-	E	M	240	1,848	62	29	43	77
VIR2	*Virola surinamensis*	Myristic-	E	T	184	3,091	64	28	276	13

[a]Nomenclature follows Garwood and Tebbs (2009).

[b]Leaf habits are evergreen (E), brevideciduous (DB), and facultatively deciduous as the dry season develops (DF).

[c]Life forms are liana (L), shrubs (S, maximum heights < 5 m), understory treelets (U, <10 m), midstory trees (M, <20 m), and canopy and emergent trees (T, >20 m).

[d]Number of rooted individuals in the 50-ha Forest Dynamics Plot in 2007 for lianas and 2005 for free-standing life forms (Condit *et al.* 2012, Schnitzer *et al.* 2012).

[e]Sample size records is the total number of trap–census combinations for each species. Sample size traps is the number of different traps that captured each species, with a maximum of 200. Sample size years is the number of species-specific phenological years between 9 February 1987 and 27 December 2016 (see *Results: Phenological censuses and the response variable*).

[f]Median first flowering dates are calculated as the median day of first flower records over species-specific phenological years and converted to a common day-of-year scale. First and last median first flowering dates refer to the phenological years with earliest and latest flowering, respectively. First, day-of-year dates are larger than last day-of-year dates for three species because their range of median first flowering dates spans the end of the calendar year.

Our analyses for the day-of-year hypothesis recreated population-level standard deviations of median first flowering censuses ($r^2 = 0.9991$, Fig. S3). We had not anticipated this result, but, in retrospect, it is inevitable because the fixed day of the year that coincides most closely with the overall median first census must minimize RMSE. For this reason, analyses of long-term phenological records cannot provide evidence for fixed photoperiodic control of phenological events unless the prediction constrains the time of year. The RMSE values calculated for our unconstrained day-of-year hypothesis equal observed population standard deviations of first flowering censuses. Small discrepancies remain between RMSE values and observed population standard deviations (Fig. S3) because years do not have an even number of seven-day census intervals (and many of our census intervals were not seven days) so that census intervals begin and end on different days of the year in different years and occasionally a fixed day of the year will fall one census interval earlier or later than expected.

Hypotheses concerning temporal variation in rainfall fared poorly (Table 3, Figs. S8–S10). The species-specific mismatch between predicted and observed flowering times averaged four censuses larger for hypotheses involving rainfall than for hypotheses involving irradiance (*cf*, RMSE values in Tables 2 and 3).

Ten species had minimum RMSE ≤ 2 for one or more of the irradiance hypotheses, and six of these had minimum RMSE ≤ 1.5 (Table 2). For five of these species, predictions from hypotheses concerning irradiance also improved on baseline

TABLE 2. *The smallest root-mean-square-error (RMSE) values and associated parameter values for each species for hypotheses concerning day of the year and maximum, mean, and directional change of irradiance. The smallest RMSE value is bolded for each species, and RMSE values within 1 unit of the smallest, species-specific RMSE value are italicized. Units are days for* N_d *and* N_e*, MJ/m*^{2} *for* T *for maximum and mean irradiance and MJ/m*^{2}*/d for* T *for directional change in irradiance.*

	Day of year		Maximum irradiance				Mean irradiance				Directional change in irradiance			
Species	RMSE	DOY_{crit}	RMSE	N_d	N_e	T	RMSE	N_d	N_e	T	RMSE	N_d	N_e	T
ALSB	**1.82**	113	*2.42*	49	93	17.75	*2.47*	40	88	18.50	4.44	111	49	0.15
BEIP	**1.76**	340	5.56	10	14	17.00	4.38	1	2	17.50	*2.72*	2	36	0.10
CORA	**1.13**	58	*1.36*	2	83	17.75	*1.39*	1	80	17.75	*1.91*	44	52	0.13
CORB	**1.27**	51	*1.89*	1	79	16.75	*1.88*	5	75	16.50	*2.07*	34	59	0.11
CORL	**0.94**	56	*1.18*	1	82	17.75	*1.26*	1	78	17.75	*1.87*	43	55	0.12
DIPP	**1.77**	168	*2.29*	107	82	17.75	*2.30*	104	83	17.75	4.72	155	53	0.13
FARO	**2.55**	140	*3.19*	78	68	18.50	*3.18*	74	70	18.50	5.22	128	60	0.11
GUSS	*1.75*	79	*1.65*	17	87	17.75	**1.59**	20	79	17.75	*2.24*	54	60	0.11
HIR1	**4.37**	69	*4.95*	24	14	20.25	*4.80*	48	1	19.50	*4.76*	65	52	0.13
HYBP	**2.43**	89	*2.96*	38	54	19.00	*2.82*	59	7	19.50	4.55	54	60	0.11
JACC	**1.89**	73	*2.22*	9	98	17.25	*2.26*	11	89	17.00	3.16	54	60	0.11
LUE1	**1.59**	15	*2.04*	2	31	17.00	*2.19*	1	28	16.75	*1.65*	14	40	0.15
MARP	*1.62*	58	**1.50**	2	93	17.25	*1.55*	3	92	17.00	*2.18*	43	55	0.12
PRIA	*2.11*	45	*1.54*	1	77	16.75	**1.50**	2	72	16.50	*2.09*	37	50	0.14
SIMA	**1.24**	46	*1.63*	1	77	16.50	*1.57*	1	71	16.50	*1.79*	35	57	0.11
TABA	**3.07**	55	*3.81*	22	7	20.25	*3.73*	17	4	20.00	*3.88*	44	52	0.13
THIM	*1.62*	18	*1.60*	2	32	17.00	*1.60*	3	31	16.75	**1.16**	15	49	0.13
TRIC	*1.20*	58	**1.18**	1	89	17.00	*1.20*	5	79	16.75	*1.62*	41	60	0.11
VIR2	**4.26**	330	8.25	10	14	17.00	7.06	13	1	16.50	*4.45*	11	17	0.17

inter-annual variation in flowering time (Table 2, RMSE values associated with an irradiance hypothesis are smaller than RMSE values associated with the day-of-year hypothesis).

We will use *Gustavia superba* to compare irradiance hypotheses and illustrate sensitivity to model parameters. *Gustavia superba* flowers in the dry season, with median first flowering censuses falling between February 16 and April 12 (Fig. 2, Table 1). The 1,000 smallest RMSE values are for hypotheses concerning mean and maximum irradiance, with no clear reason to prefer one hypothesis over the other (Fig. 3). RMSE values are highly sensitive to values of N_e, N_d, and T (Fig. 4). Minimum RMSE values occur when large mean irradiance values of 17 to 18 MJ/m^2 (T) are maintained for 80 to 120 days (N_e) shortly before median first flowering dates (Table 2; Fig. 4, lower panels for $N_d = 1$ and $N_d = 10$). The predictions of the mean and maximum irradiance hypotheses converge when N_e is large, and it is not surprising that they cannot be distinguished for N_e values between 80 and 120 days. Figures S1 and S4–S10 present the same information for all 19 species for all six rainfall and irradiance hypotheses.

Just two of the six models concerning rainfall and irradiance hypotheses were associated with RMSE ≤ 2. The hypothesis that increasing irradiance cues flowering was consistent with observed flowering times for *Luehea seemannii* and *Thinouia myriantha*. For both species, flowers develop in about two weeks (N_d) after six or seven weeks (N_e) of sustained rapid increase in irradiance of 0.13 or 0.15 MJ/m^2/d (Table 2).

The hypothesis that a sustained period of high irradiance triggered flowering was consistent with observed flowering times (i.e., RMSE ≤ 2) for eight species. The three species of *Cordia* exemplify this outcome. Flowers of all three *Cordia* species develop in just 1 to 5 days (N_d in Table 2) after 75 to 83 days (N_e) in which mean and maximum irradiance were very high (>16.5 MJ/m^2 for *C. bicolor* and >17.75 MJ/m^2 for *C. alliodora* and *C. lasiocalyx, cf* Fig. 1). *Gustavia superba, Maripa panamensis, Prionostemma asperum, Simarouba amara*, and *Triplaris cummingiana* have similar values of N_d, N_e, and T, with the very large flowers of *Gustavia* taking slightly longer to develop (Table 2). The predictions of the mean and maximum irradiance hypotheses converge for large N_e (see *Methods: Phenological hypotheses and analyses*), and our interpretation is that sustained high irradiance cues flowering for these eight species. We also infer that the sustained high levels of irradiance release resting reproductive buds because flower development times are consistently short in these eight species.

DISCUSSION

We used median first flowering observations recorded from 30 years of weekly censuses of 200 passive traps and concurrent meteorological measurements to evaluate six possible proximate cues for flowering in 19 annually flowering species. Inter-annual variation in first flowering times differed widely among species (Table 1, Fig. S1). Over the 30 years of observation, median first flowering dates spanned just 27 and 29 calendar days for *Cordia*

TABLE 3. *The smallest root-mean-square-error (RMSE) values and associated parameter values for each species for hypotheses concerning maximum, mean, and directional change of rainfall. Not one RMSE value falls within 1 unit of the smallest species-specific RMSE values observed for hypotheses concerning day of the year and maximum, mean, and directional change of irradiance (see Table 2). Units are days for* N_d *and* N_e*, mm for* T *for maximum and mean daily rainfall, and mm/d for* T *for directional change in rainfall.*

	Maximum daily rainfall				Mean daily rainfall				Directional change in rainfall			
Species	RMSE	N_d	N_e	T	RMSE	N_d	N_e	T	RMSE	N_d	N_e	T
ALSB	7.10	179	17	17	7.39	209	125	9.2	5.70	6	32	0.3
BEIP	3.73	92	115	5	3.73	54	58	5.6	20.6	18	60	0.2
CORA	4.74	116	4	28	8.32	201	125	9.1	4.17	142	8	1.6
CORB	4.28	114	2	36	9.02	210	125	8.5	3.60	116	27	0.3
CORL	4.79	116	4	28	8.15	201	125	9.1	4.14	143	5	1.8
DIPP	11.2	10	1	62	11.0	206	125	9.7	7.38	5	32	0.4
FARO	8.83	180	17	17	8.96	210	123	9.3	6.06	6	32	0.3
GUSS	6.61	115	5	24	7.68	210	125	8.5	5.35	186	8	1.6
HIR1	7.68	115	2	36	7.94	210	125	8.5	5.86	186	8	1.6
HYBP	6.50	166	16	17	6.54	209	124	9.1	6.94	172	8	1.9
JACC	6.03	116	4	28	7.20	210	125	8.5	4.90	142	8	1.6
LUE1	4.22	111	2	34	10.4	209	122	6.0	2.68	124	2	0.9
MARP	5.15	116	4	28	8.16	201	125	9.1	4.31	142	8	1.6
PRIA	5.29	111	4	28	9.41	207	124	8.8	4.02	93	18	0.4
SIMA	4.59	111	4	28	9.02	201	125	9.1	3.41	143	5	1.4
TABA	5.21	115	2	34	7.98	210	125	8.5	4.78	116	27	0.3
THIM	5.47	111	4	28	9.97	209	124	5.9	2.39	127	1	1.6
TRIC	4.96	116	4	28	8.31	207	124	8.8	4.08	143	5	1.8
VIR2	6.59	145	53	5	6.41	103	93	7.1	19.4	24	44	0.3

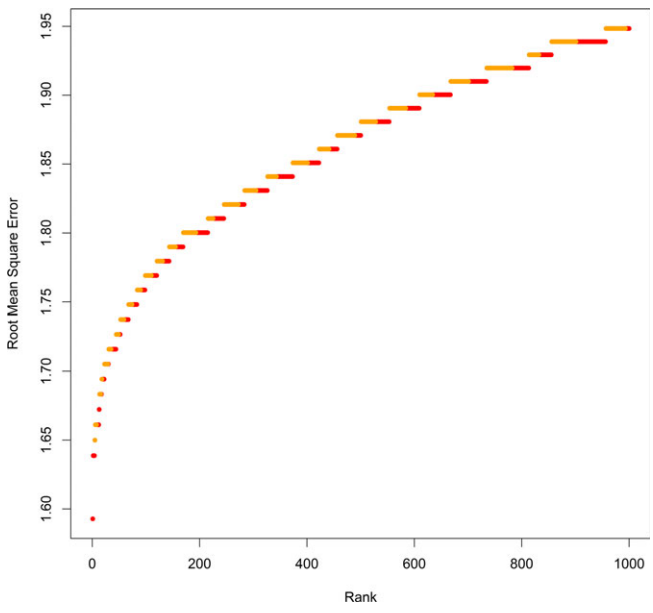

FIGURE 3. For *Gustaiva superba,* the 1000 smallest root-mean-square-error (RMSE) values were for phenological models concerning mean (red) and maximum (orange) irradiance. Figure S4 presents the same information for all 19 study species.

lasiocalyx and *Simarouba amara*, respectively; 55 days for the median species; and 102 and 121 days for *Virola surinamensis* and *Hirea reclinata*, respectively (Table 1, Fig. S1). The large interannual variation observed for the timing of the onset of flowering suggests that photoperiodic cues are unlikely to control the timing of flowering in most species.

There is an additional reason to doubt one class of photoperiodic cue. Solar insolation at the top of the atmosphere is hypothesized to serve as a proximate cue for tropical plant phenology and, like photoperiod, is controlled by solar declination (Calle *et al.* 2009, 2010, Borchert *et al.* 2015). It is unclear how plants sense solar insolation at the top of the atmosphere. At the latitude of BCI (9° 10′ N), top-of-the-atmosphere insolation has two annual maxima with similar irradiance (≈433 W/m^2) near the equinoxes, a minor minima near the summer solstice (422 W/m^2) and an overall minima near the winter solstice (361 W/m^2). The seasonality of solar irradiance experienced by the BCI forest (Fig. 1) bears no resemblance to the seasonality of top-of-the-atmosphere insolation because atmospheric transmissivity varies seasonally. The seasonal movements of the Intertropical Convergence Zone bring alternating cloudy and sunny seasons to BCI and to most tropical forests. Clouds absorb photosynthetically active radiation, and alternating cloudy and sunny seasons cause differences in atmospheric transmissivity that

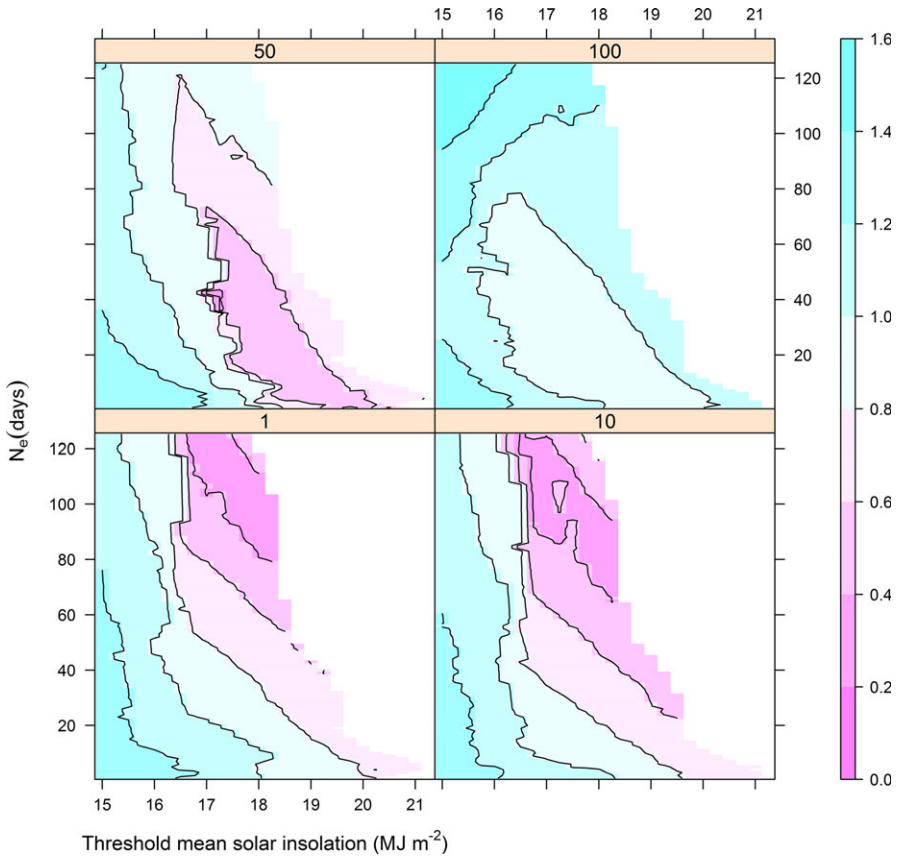

FIGURE 4. Contour plots of base 10 logarithms of root-mean-square-error (RMSE) values over parameter sets defining the phenological model relating inter-annual variation in the timing of flowering to changes in mean levels of irradiance for *Gustavia superba*. The model predicts first flowering occurs N_d days after the first time cumulative irradiance over the prior N_e days exceeds a threshold level T each year. Each panel presents a single value of N_d (1, 10, 50 or 100 days), all integer values of N_e between 1 and 125, and all values of T between 15 and 21 MJ/m^2 with 0.25 MJ/m^2 steps. Blank, white regions to the right of each panel correspond to large values of N_e and T that occurred in fewer than 27 years and are therefore excluded. Figure S5 presents the same information for all 19 study species. Figures S6–S10 present the same information for the five remaining environmental hypotheses and all 19 study species.

overwhelm seasonal differences in top-of-the-atmosphere insolation for many tropical forests. This is particularly true at low latitudes where seasonality of top-of-the-atmosphere insolation is limited. As an example, the single-day maximum top-of-the-atmosphere insolation is only 19.9 percent larger than the single-day minimum at 9° 10′ N; yet, the BCI forest averages 49.9 percent more solar irradiance for 50 consecutive dry-season days (from 17 February through 6 April) than for 178 consecutive wet-season days (from 1 June through 30 November) (Fig. 1). We conclude that the timing of flowering on BCI is insensitive to top-of-the-atmosphere insolation (Zimmerman *et al.* 2007).

The large inter-annual variation in the timing of the onset of flowering (Table 1, Fig. S1) offers ample opportunity to evaluate relationships with inter-annual variation in potential environmental cues. We documented consistently poor matches between inter-annual variation in the timing of flowering and the timing of rainfall seasonality (Table 3, Figs. S8–S10). This is consistent with an earlier experimental study and extends the interpretation of that experiment. The timing of leaffall and flowering was unaffected for many of the same species in a forest irrigation experiment that maintained soil water potentials at field capacity (i.e., above −0.05 MPa) for 2.25-ha plots for five consecutive dry seasons (Wright & Cornejo 1990a,b). Although the irrigation treatment successfully eliminated soil drought, relative humidity in the upper canopy was unaffected and the possibility that canopy species responded to atmospheric drought but not soil drought could not be discounted (Wright & Cornejo 1990a,b). The present study now allows us to discount atmospheric drought. Inter-annual variation in the timing of rainfall seasonality affects moisture availability in both the atmosphere and the soil and does not predict the timing of flowering in the 19 BCI species studied here.

A second irrigation experiment provides a counter-example and a cautionary note for the interpretation of the results of the present study. Continuous irrigation supplied from the end of the rainy season suppressed dry-season flowering in *Hybanthus prunifolius* while, after eight rainless weeks without irrigation, a single application of as little as 5 mm of water stimulated flowering

(Augspurger 1982). A similar prior drought stress is required before rain or irrigation can successfully stimulate flowering in *Coffea arabica* (Carr 2001) and might play a role in the general flowering phenomenon that characterizes the aseasonal Dipterocarp forests of South-East Asia (Sakai *et al.* 2006). Our analyses failed to detect an association between flowering and rainfall in *H. prunifolius* (Table 3, Figs. S8–S10) because our phenological models omitted a prior drought stress requirement and predicted early flowering near the beginning of the dry season in most years. The forest irrigation experiment described in the previous paragraph provided continuous irrigation from the end of the rainy season and did not alter flowering times; however, *H. prunifolius* was not studied in the forest irrigation experiment (Wright & Cornejo 1990a,b). We conclude that rain following dry-season drought cues flowering in *H. prunifolius*, but not in the remaining 18 species studied here.

Hypotheses concerning inter-annual variation in irradiance predicted flowering times successfully for 10 of the 19 study species (see *Results: Phenology hypotheses*). For eight species, flowering follows quickly after 10 to 12 weeks of consistent, high levels of irradiance at the forest canopy. For the two remaining species, flowering follows two weeks after six or seven weeks of sustained increases in irradiance at the forest canopy. The timing of first flowering correlates well with the timing of sustained seasonal increases in irradiance in these 10 species. We conclude that seasonal changes in irradiance are the proximate cues for flowering for these and possibly other BCI species. The physiological mechanisms linking levels of irradiance and flowering are unknown, but might involve threshold levels of carbohydrate reserves. Our next steps will be to build new phenological models to explore additional hypotheses, for example, a prior drought requirement, and to build new types of models able to address the many species that flower continuously or with multiple modes within a year in moist tropical forests.

ACKNOWLEDGMENTS

We thank Helene Muller-Landau for extensive discussions that improved our analyses. The Environmental Sciences Program of the Smithsonian Institution funded this study from 1987 to 2003. The Smithsonian Tropical Research Institute continued funding since 2003.

DATA AVAILABILITY

Data available from the Dryad Digital Repository: https://doi.org/10.5061/dryad.7n77q (Wright & Calderón 2017).

SUPPORTING INFORMATION

Additional Supporting Information may be found online in the supporting information tab for this article:

FIGURE S1. The seasonal timing of flowering for 19 study species identified by bold four letter codes.

FIGURE S2. Box plots of annual values of numbers of traps that captured flowers for each phenological year for the 19 study species.

FIGURE S3. The relationship between the population-level standard deviation of observed median first flowering censuses and the root-mean-square error calculated for first flowering censuses predicted by the day-of-year hypothesis and observed median first flowering censuses.

FIGURE S4. The 1000 smallest root-mean-square-error values for 19 study species identified by bold four letter codes.

FIGURE S5. Contour plots of base 10 logarithms of root-mean-square-error values over parameter sets defining the phenological model relating changes in mean levels of irradiance to the timing of flowering for 19 study species identified by bold four letter codes.

FIGURE S6. Contour plots of base 10 logarithms of root-mean-square-error values over parameter sets defining the phenological model relating changes in maximum levels of irradiance to the timing of flowering for 19 study species identified by bold four letter codes.

FIGURE S7. Contour plots of base 10 logarithms of root-mean-square-error values over parameter sets defining the phenological model relating directional changes in levels of irradiance to the timing of flowering for 19 study species identified by bold four letter codes.

FIGURE S8. Contour plots of base 10 logarithms of root-mean-square-error values over parameter sets defining the phenological model relating changes in mean levels of daily rainfall to the timing of flowering for 19 study species identified by bold four letter codes.

FIGURE S9. Contour plots of base 10 logarithms of root-mean-square-error values over parameter sets defining the phenological model relating changes in maximum levels of daily rainfall to the timing of flowering for 19 study species identified by bold four letter codes.

FIGURE S10. Contour plots of base 10 logarithms of root-mean-square-error values over parameter sets defining the phenological model relating directional changes in daily rainfall to the timing of flowering for 19 study species identified by bold four letter codes.

LITERATURE CITED

Aide, T. M. 1993. Patterns of leaf development and herbivory in a tropical understory community. Ecology 74: 455–466.

Ashton, P. S., T. J. Givnish, and S. Appanah. 1988. Staggered flowering in the Dipterocarpaceae - new insights into floral induction and the evolution of mast fruiting in the aseasonal tropics. Am. Nat. 132: 44–66.

Augspurger, C. K. 1982. A cue for synchronous flowering. *In* A. S. R. Egbert Giles Leigh Jr, and D. M. Windsor (Eds). The ecology of a tropical forest, pp. 133–150. Smithsonian Institution Press, Washington, DC

Borchert, R., Z. Calle, A. H. Strahler, A. Baertschi, R. E. Magill, J. S. Broadhead, J. Kamau, J. Njoroge, and C. Muthuri. 2015. Insolation and photoperiodic control of tree development near the equator. New Phytol. 205: 7–13.

Calle, Z., B. O. Schlumpberger, L. Piedrahita, A. Leftin, S. A. Hammer, A. Tye, and R. Borchert. 2010. Seasonal variation in daily insolation

induces synchronous bud break and flowering in the tropics. Trees-Struct. Funct. 24: 865–877.

Calle, Z., A. H. Strahler, and R. Borchert. 2009. Declining insolation induces synchronous flowering of Montanoa and Simsia (Asteraceae) between Mexico and the Equator. Trees-Struct. Funct. 23: 1247–1254.

Carr, M. K. V. 2001. The water relations and irrigation requirements of coffee. Exp. Agric. 37: 1–36.

Condit, R., S. Lao, R. Pérez, S. B. Dolins, R. B. Foster, and S. P. Hubbell. 2012. Barro Colorado Forest Census Plot Data, 2012 Version. DOI http://doi.org/10.5479/data.bci.20130603.

Croat, T. B. 1978. Flora of Barro Colorado Island. Stanford University Press, Stanford, California.

Garwood, N. C., and M. C. Tebbs. 2009. Seedlings of Barro Colorado Island and the neotropics. In association with the Natural History Museum, London, UK.

Leigh Jr, E. G. 1999. Tropical forest ecology: a view from Barro Colorado Island. Oxford University Press, Oxford, UK.

Leigh Jr, E. G., and D. M. Windsor. 1982. Forest production and regulation of primary consumers on Barro Colorado Island. *In* E. G. Leigh Jr, A. S. Rand, and D. M. Windsor (Eds.). The ecology of a tropical forest, pp. 111–122. Smithsonian Institution Press, Washington, DC.

Linkosalo, T., H. K. Lappalainen, and P. Hari. 2008. A comparison of phenological models of leaf bud burst and flowering of boreal trees using independent observations. Tree Physiol. 28: 1873–1882.

Njoku, E. 1959. Response of rice to small differences in length of day. Nature 183: 1598–1599.

Primack, R. B. 1985. Longevity of individual flowers. Annu. Rev. Ecol. Syst. 16: 15–37.

Reich, P. B., and R. Borchert. 1982. Phenology and ecophysiology of the tropical tree, *Tabebuia neochrysantha* (Bignoniaceae). Ecology 63: 294–299.

Reich, P. B., and R. Borchert. 1984. Water stress and tree phenology in a tropical dry forest in the lowlands of Costa Rica. J. Ecol. 72: 61–74.

Sakai, S., R. D. Harrison, K. Momose, K. Kuraji, H. Nagamasu, T. Yasunari, L. Chong, and T. Nakashizuka. 2006. Irregular droughts trigger mass flowering in aseasonal tropical forests in Asia. Am. J. Bot. 93: 1134–1139.

Satake, A., T. Kawagoe, Y. Saburi, Y. Chiba, G. Sakurai, and H. Kudoh. 2013. Forecasting flowering phenology under climate warming by modelling the regulatory dynamics of flowering-time genes. Nat. Commun. 4: 2303.

van Schaik, C. P., J. W. Terborgh, and S. J. Wright. 1993. The phenology of tropical forests: adaptive significance and consequences for primary consumers. Annu. Rev. Ecol. Syst. 24: 353–377.

Schnitzer, S. A., S. A. Mangan, J. W. Dalling, C. A. Baldeck, S. P. Hubbell, A. Ledo, H. Muller-Landau, M. F. Tobin, S. Aguilar, D. Brassfield, A. Hernandez, S. Lao, R. Perez, O. Valdes, and S. R. Yorke. 2012. Liana abundance, diversity, and distribution on Barro Colorado Island, Panama. PLoS ONE 7: e52114. https://doi.org/10.1371/journal.pone.0052114

Tutin, C. E. G., and M. Fernandez. 1993. Relationships between minimum temperature and fruit production in some tropical forest trees in Gabon. J. Trop. Ecol. 9: 241–248.

Wright, S. J., and O. Calderon. 1995. Phylogenetic patterns among tropical flowering phenologies. J. Ecol. 83: 937–948.

Wright, S. J., and O. Calderon. 2006. Seasonal, El Nino and longer term changes in flower and seed production in a moist tropical forest. Ecol. Lett. 9: 35–44.

Wright, S. J., and O. Calderón. 2017. Data from: Solar irradiance as the proximate cue for flowering in a tropical moist forest. Dryad Digital Repository. https://doi.org/10.5061/dryad.7n77q

Wright, S. J., and F. H. Cornejo. 1990a. Seasonal drought and leaf fall in a tropical forest. Ecology 71: 1165–1175.

Wright, S. J., and F. H. Cornejo. 1990b. Seasonal drought and the timing of flowering and leaf fall in a neotropical forest. *In* K. S. Bawa, and M. Hadley (Eds.). Reproductive ecology of tropical forest plants, pp. 49–61. UNESCO and the Parthenon Publishing Group, Paris, France.

Wright, S. J., H. C. Muller-Landau, R. Condit, and S. P. Hubbell. 2003. Gap-dependent recruitment, realized vital rates, and size distributions of tropical trees. Ecology 84: 3174–3185.

Wright, S. J., and C. P. van Schaik. 1994. Light and the phenology of tropical trees. Am. Nat. 143: 192–199.

Wycherley, P. R. 1973. The phenology of plants in the humid tropics. Micronesica 9: 75–96.

Yeang, H. Y. 2007. Synchronous flowering of the rubber tree (*Hevea brasiliensis*) induced by high solar radiation intensity. New Phytol. 175: 283–289.

Zimmerman, J. K., S. J. Wright, O. Calderon, M. A. Pagan, and S. Paton. 2007. Flowering and fruiting phenologies of seasonal and aseasonal neotropical forests: the role of annual changes in irradiance. J. Trop. Ecol. 23: 231–251.